Delft University of Technology

Efficient Sparse Street Furniture Extraction from Mobile Laser Scanning Point Clouds

Truong-Hong, L.; Lindenbergh, R. C.; Vermeij, M. J.

Citation (APA)
Truong-Hong, L., Lindenbergh, R. C., & Vermeij, M. J. (2022). Efficient Sparse Street Furniture Extraction from Mobile Laser Scanning Point Clouds. *International Archives of the Photogrammetry, Remote Sensing and Spatial Information Sciences - ISPRS Archives*, *48*(4/W4-2022), 161-168. https://doi.org/10.5194/isprs-archives-XLVIII-4-W4-2022-161-2022

Important note
To cite this publication, please use the final published version (if applicable).
Please check the document version above.

EFFICIENT SPARSE STREET FURNITURE EXTRACTION FROM MOBILE LASER SCANNING POINT CLOUDS

L. Truong-Hong [1*], R.C. Lindenbergh [1], M.J. Vermeij [2],

[1] Dept. of Geoscience & Remote Sensing, Delft University of Technology, Delft, The Netherlands, - (l.truong; r.c.lindenbergh)@tudelft.nl
[2] Municipality of Rotterdam City Management Basic information, The Netherlands, - mj.vermeij@rotterdam.nl

Commission IV, WG IV/9

KEY WORDS: Point Cloud, Cells, Sub-cell, Voxel, Voxel-Based Region Growing, Kernel Density, Surface Extraction, object identification

ABSTRACT:

Current mobile systems are capable of efficiently acquiring dense urban point clouds. Still, operational use of such data is hampered by the lack of efficient object extraction methodology. Notably methodology is lacking for automatically extracting objects that do not belong to the road furniture like street signs and light poles but do belong to the street furniture. As an example, object we consider public garbage bins, that are installed and should be maintained in public areas in every city. However, information about types, locations, and condition of these public garbage bins are rarely updated and only obtained through manual measurements. Therefore, an efficient way of collecting information on such public objects is of interest not only for urban management but also when developing digital twins of a city. This study proposes a new method to automatically extract public garbage bins from large urban mobile laser scanning (MLS) point clouds. The proposed method consists of three main steps: (1) cell-, (2) sub-cell-, and (3) surface-based filtering, in which both spatial information of the point clouds and contextual knowledge of the public garbage bins are incorporated to efficiently remove irrelevant 3D points at an early phase and identify and classify different types of public garbage bins. Contextual knowledge includes shape and dimensions, and the relationship between the public garbage bins and the ground surface. A MLS dataset of the city centre of Rotterdam, the Netherlands, consisting of 2.84 billion points organised in 166 tiles of 50 x 75m, and covering an area of about 750 x 750m was used to test the proposed method. Results show that the method can automatically extract ~90 public garbage bins with an overall detection rate of 89.1%. Moreover, the executing time for the entire dataset was only about 163.6 minutes, which is equivalent to 3.46 seconds per one million points. Although the method was tested here one public garbage bins, it can be easily tuned for the detection of other street furniture objects, like benches, post boxes or bollards.

1. INTRODUCTION

A mobile laser scanner (MLS) system integrated into a moving vehicle (e.g., car, train or boat) can acquire three-dimensional (3D) topographic information of visible surfaces of objects along the route of the vehicle. Because of its high point density with an accuracy in the centimetre range, MLS data have become a resource for documenting 3D objects and assessing the state of objects (Pu et al., 2011). Results of those tasks can be integrated into a smart city concept, and BIM environments and digital twins (DT) of a city (Shirowzhan et al., 2020).

In the light of creating digital models or DT of a city, MLS point clouds have been used to extract building facades (Zhou et al., 2018), road surfaces (Yadav et al., 2017), traffic and light poles (Wang et al., 2017), and trees (Weinmann et al., 2017). However, other urban utilities along the road environment, for example, telephone boxes, electricity control boxes, and public garbage bins, have received less attention, although these objects belong to a digital model of a city, and in addition require maintenance by municipalities. This lack of attention may be caused because the extraction of relatively sparse objects is still challenging. Reason could be a lack of training data for extracting such objects with machine leaning methods and the geometric complexity and variability of these objects. In the DT of a city, both geometric models and semantic information of all physical assets must be included. As such, to complement existing work toward providing geometric models for DTs, this study proposes an automatic method to extract point clouds of public garbage bins installed along the city streets from MLS data. Resulting point clouds can be subsequently used to not only identify type,

location, and conditional status of the public garbage bins, but also to create 3D models for integration in a DT, and asset management. Here we like to emphasize that public garbage bins are chosen to showcase the methodology, but that the method is expected to work equally well on similar urban utility objects.

2. RELATED WORK

A mobile laser scanner installed on a vehicle captures 3D topographic information of objects surfaces along streets. Such data are subsequently used to obtain geometric and semantic information of urban objects, which includes building facades, road surfaces and road signs, poke-like objects (light poles and traffic lights) and trees along the streets. Existing methods are mostly focussing to obtain geometric point clouds of roads and road facilities (e.g., traffic and light poles) by using geometric features derived from MLS point clouds and/or machine learning or hybrid methods. As such, this survey roughly classifies these methods based on physical assets extracted from the point clouds, which include road surfaces and their boundaries, road marking, poke-like objects, and trees.

In extracting road surfaces and reconstructing road boundaries, Yadav et al. (2017) proposed three consequent steps to obtain final points of the road surface. First, intensity and point density were applied to extract ground points from MLS data. Second, region growing based height and intensity difference was applied to remaining points to obtain points of the road surface. Finally, a smooth road boundary was created from the points of the extracted road surface, which was then used to eliminate incorrect points along the road boundary. Zai, et al. (2018)

---

* Corresponding author

decomposed 3D point clouds into voxels to segment the data points into facets by using the tangent plane and smoothness of points. Subsequently, the points on the road boundary were extracted by the alpha-shape algorithm (Edelsbrunner et al., 1983), while graph cut-based energy minimization was implemented to refine the road boundary.

Additionally, from the points of the road surfaces, the road marking was extracted using clustering techniques based on the intensity values of the data points (Soilán et al., 2017). These approaches were applied directly to data points (Yang et al., 2018) or indirectly through an intensity image created from the point cloud (Soilán et al., 2017). Different road markings were achieved based on analysing geometric features (e.g., length, width, and area, etc.) of the clusters (Soilán et al., 2017). Interestingly, deep learning has been employed to detect and classify road markings based on raster images, for example, Tian et al. (Tian et al., 2018) used a modified Faster R-CNN and Wen et al. (Wen et al., 2019) used a Generative Adversarial Network (GAN). In the work of Wen et al. (2019), a context-based method is used to add missing road marking, while Bai et al. (2021) used the 3D deep learning method RandLA-Net, to provide a full functional classification of road surfaces, including road lanes, bicycle paths and pavements.

MLS data is also used to extract poke-like objects including light poles, traffic lights and trees. Liu et al. (2020) extracted pole-like objects by identifying point in arc-like configurations in cross-sections using RANSAC while analysis of eigenvalues and principal directions was implemented to classify objects as lamp posts, traffic lights and traffic signs. Yadav et al. (2022) classified pole and non-pole like objects from non-ground point clusters using random forest with features including height, area, eigenvalues, linearity, planarity, and sphericity. Additionally, Wang et al. (2021) roughly extracted rod-shaped parts of pole-like objects based on the vertical continuity of voxels generated from non-ground points, while the random forest model was used to classify the pole-like objects based on local- and global-scale features. Shi et al. (2018) extracted pole like objects based on cylindrical or linear feature detection followed by shape matching between the point clouds of extracted objects and templates to classify each cluster as street lamp, traffic sign, or utility pole.

Furthermore, tree extraction from MLS data has attracted attention from many researchers. Zhong, et al. (2017) clustered candidate points of trees based on octree's nodes connectivity, in which an octree was generated from a subset after removing data points of building facades and road surfaces. Subsequently, the histogram-based octree's nodes were used to detect a stem while overlapping canopy segmentation was used to separate a tree from its neighbour. Similarly, Weinmann et al. (2017) used a random forest to classify MLS point clouds based on a set of point-based features computed by using principal component analysis with different neighbourhood scales. A mean shift segmentation was used to cluster the points of individual trees while shape analysis was employed to remove unreal trees. Interestingly, Guan et al. (2015) extracted MLS points of individual trees using Euclidean distance clustering from non-ground points, while deep learning was applied to artificial waveforms of tree clusters generated in vertical direction for tree classification. Also using a deep learning framework, Luo et al. (2021) developed a pointwise direction embedding deep network (PDE-net) to predict direction vectors of tree's points to enhance the boundary of the tree, in which the tree's points were obtained using an Euclidean distance clustering approach. Each cluster

was classified as single or multi-tree cluster based on the number of detected tree centres. Subsequently, region growing and the embedded pointwise directions were used to decompose a multi-tree cluster into single tree clusters corresponding to individual s ingle tree.

In summary, existing methods are mainly focussing in extracting the main objects (e.g., road surface, light poles, and traffic poles) of urban streets. These methods mostly use point features to extract objects of interest, which requires intensive computational resources, as typically properties of all individual points are required. Moreover, other utilities along urban streets, for example telecom and electricity control boxes or public garbage bins have not yet received attention in research and practical point cloud based urban management. As such, this study proposes a new method to automatically extract point clouds of public garbage bins installed along urban streets from MLS data.

3. PROPOSED METHOD

As data points of public garbage bins often account for only a small percentage of an entire urban 3D point cloud, the use of features of data points may require intensive computation. Moreover, it would be difficulty to establish thresholds to distinguish point clouds of the public garbage bins from others. As such, this study proposes a new method combining spatial point cloud information and contextual knowledge to extract the points of the public garbage bins in three consecutive steps. *Step 1*, cell-based filtering aims to retrieve 2D cells in the xy plane, which possibly contain points of the public garbage bins, which also enables the quick elimination of many unneeded points. *Step 2*, sub-cell-based filtering extracts cluster points of vertical surfaces of the garbage bins. Finally, *Step 3* employs a segmentation method to extract points of surfaces from the cluster points, and identifies if the cluster is a public garbage bin and of what type (Figure 1). In each step, contextual knowledge is integrated to (1) roughly extract a subset containing data points of the garbage bin, and (2) to eliminate incorrect clusters or surfaces of the public garbage bins.
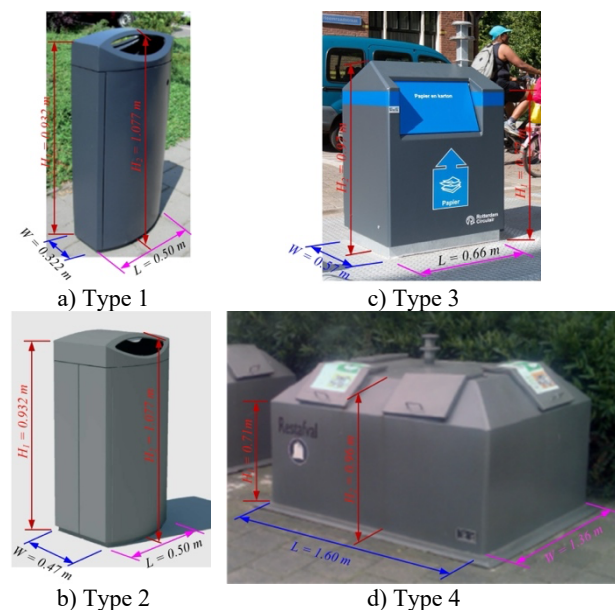

| a) Type 1 | c) Type 3 |
| b) Type 2 | d) Type 4 |

Figure 1. Public garbage bins used in Rotterdam city, The Netherland

3.1 Contextual knowledge

As the proposed method is tested to extract public garbage bins along urban streets of Rotterdam city, The Netherlands, contextual knowledge derived from configuration and geometric features of the public garbage bins in this city is incorporated into the proposed method (Figure 2). The contextual knowledge herein includes lower and upper bounds of dimensions of the garbage bin, and a relationship between surfaces of the garbage bin and these surfaces and a ground surface. Following features obtained from designed documents and available points clouds of garbage bins are used in this study.

Feature 1: A public garbage bin is installed on top of a flat ground surface, but there is often a small gap between vertical surfaces of the garbage bin and the ground surface.

Feature 2: As the MLS scanning line is often perpendicular to the road central line, geometries of only a front and/or two side surfaces of the public garbage bins are usually captured. As such, point clouds of two or three vertical surfaces are available. The points of each vertical surface continuously distribute in the vertical direction from the ground level.

Feature 3: As alignment error and noisy data are inevitable, dimensions of the garbage bin based on its point cloud can be different those from the design document. In this study, the tolerance is added to compensate to an accumulate error of data.
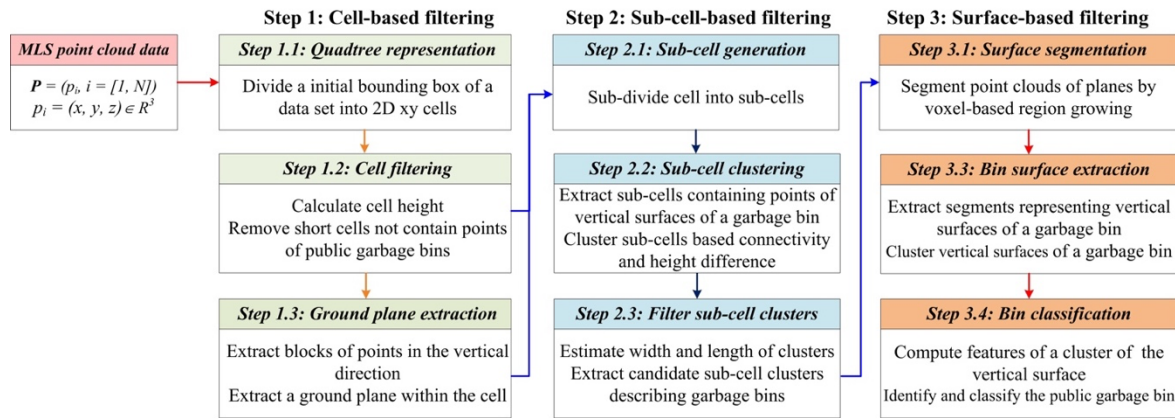

Figure 2. Workflow of the proposed method to extract recycle bins

Step 1: Cell-based filtering

Step 1 starts with *Step 1.1* employs a cell grid to divide an initial bounding box of MLS data points ($P = \{p_i = (x_i, y_i, z_i) \in R^3, i = [1, N]\}$) into smaller 2D cells ($C = \{c_i\}, i = [1, N_c]$) in the xy plane, in which the cell size is equal to a predefined cell size (ce_0). Next, *Step 1.2* roughly eliminates cells that do not possess data points of side surfaces of the garbage bin, which are the cells have heights less than the minimum height ($B.H_{min}$) of the garbage bin (Eq. 1).

$$c_j.H = max(p_j.z) - min(p_j.z) \qquad (1)$$

where $p_j.z = z$ coordinate of the point $p_j \in c_j$.

Subsequently, *Step 1.3* extracts candidate points of the vertical surfaces of the garbage bins within each remaining cell c_i. Vertical blocks (cb_{ij}) of points within each cell (c_i), in which the distance between two consecutive points is no larger than the threshold $D.g_0$, are extracted. The cell c_i is considered for further processing if it has at least one cell block having the height no less than $B.H_{min}$, in which Eq. 1 is used to compute the cell block height. Next, a valley-peak-valley pattern (Truong-Hong and Lindenbergh, 2022b) based on kernel density estimation (KDE) (Laefer and Truong-Hong, 2017) generated from $p_j.z \in c_i$ is applied to extract points of horizontal planes ($s_{ij} = (p_{ij,0}, n_{ij})$), in which principal component analysis (PCA) was used to estimate the plane parameters. Finally, the ground plane ($s_{g,i}$) is the plane satisfying Eq. 2:

$$s_{ij} \to s_{g,i} \, if \begin{cases} \angle n_{ij} n_z \leq \alpha_{g,0} \\ p_{ij,0}.z \to \min \, and \, s_{ij}.area \to \max \end{cases} \qquad (2)$$

where $s_{ij}.area$ = an area of a convex hull created from $p_{ij} = \{x, y\} \in s_{ij}$

n_z = the unit vector of the z axis

$\alpha_{g,0}$ = the maximum angle of the ground surface

a) Data points within a cell   b) Points of a block within a cell   c) Resulting ground point cloud (in red)
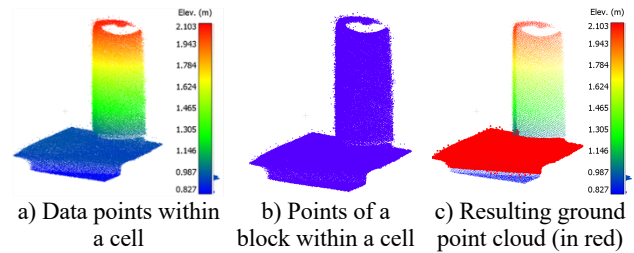
Figure 3. Extracting ground points within a cell
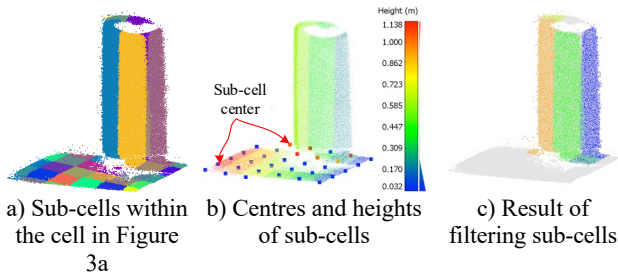
Step 2: Sub-cell-based filtering

As a cell c_i may contain points of a garbage bin and other adjacent objects (e.g., a bike and light pole), the cell c_i is again subdivided into smaller cells $sc_{ij} = \{p_{ij}\}$ (*Step 2.1*), in which a sub-cell size (sce_0) equal to $1/10 ce_0$ is used. Next, each sub-cell $sc_{ij} \in c_i$ is considered to represent a part of the vertical surface of the garbage bin if the points $p_{ij} \in sc_{ij}$ satisfy Eq. 3, which reflects that the garbage bin installed on the ground.

$$sc_{ij} = \{p_{ij}\} \, if \begin{cases} min\left(d(p_{ij}, s_{g,i})\right) \leq D.g_0 \\ max\left(d(p_{ij}, s_{g,i})\right) \leq B.H_{max} \end{cases} \qquad (3)$$

where $d(p_{ij}, s_{g,i})$ = distances from the points p_{ij} to the ground plane $s_{g,i}$

$B.H_{max}$ = the maximum height of the public garbage bins.

---

* Corresponding author

a) Sub-cells within the cell in Figure 3a

b) Centres and heights of sub-cells

c) Result of filtering sub-cells

Figure 4. Extract sub-cells representing vertical surfaces

Next, *Step 2.2* groups remaining sub-cells sc_{ij} into a set of regions $R = (R_i, i = [1, N_b], R_i = \{sc_{ij}\})$, and each cluster represents vertical surfaces of one garbage bin. The process randomly selects an initial sub-cell sc_{ij} to search adjoined neighbouring sub-cells sc_{kl} and adds to the region if the different height of the sub-cells is no more than a predefined height threshold (ΔH_{sc}). The process is completed when all sub-cells are checked.

Additionally, *Step 2.3* estimates 2D minimum bounding box in the xy plane of the cluster R_i to determine its width and length. The cluster R_i is roughly considered as the candidate garbage bin if the cluster width and length are within tolerances of lower and upper bounds of dimensions of the public garbage bins.

Step 3: Surface-based filtering

Step 3 consisting of 3 sub-steps aims to extract data points of vertical surfaces from the sub-cell cluster R_i and then identifies if the R_i is the garbage bin. *Step 3.1*, is employed voxel-based region growing (VRG) (Truong-Hong and Lindenbergh, 2022a) to segment the data points of the sub-cell cluster $R_i = \{S_{b,i}, i = [1, N_s]\}$. VRG is used a voxel grid to decomposing the points of the cluster R_i into multiple connected voxels (v_i) with the voxel size (ve_0), and the data points $p_{vi} \in v_i$ assuming to represent a plane $vs_i = (vp_{s0,i}, vn_i)$, in which $vp_{si,0}$ is the centroid of the points, the normal vector vn_i is estimated using PCA. Notably, the voxel is considered for segmentation if the number of points within the voxel is larger than a predefined threshold v_{min_ptc}. Adjoined voxels (v_i and v_j) are considered to belong to the same segment $S_{b,i}$ if the angle between normal vectors (vn_i and vn_j) and a distance ($d(vp_{s0,j}, vs_i)$) between vs_i and vs_j are less than both angle ($v\alpha_0$) and distance (vd_0) thresholds. Moreover, the voxel v_i is selected as the seeding voxel if the residual of a fitting plane of $p_{vi} \in v_i$ is no larger than the residual threshold ($vres_0$). Details of the VRG can refer to (Truong-Hong and Lindenbergh, 2022a).

Next, *Step 3.2* aims to determine vertical surfaces of the garbage bin from a set of segmented planes ($S_{b,i}$) through a following procedure. First, a fitting plane ($S_{b,i} \rightarrow s_{bi} = (p_{bi,0}, n_{b,i})$), and the width ($S_{b,i}.W$) and length ($S_{b,i}.L$) are estimated. The segment $S_{b,i}$ classifies as a vertical plane ($S_{bv,i}$), a candidate vertical surface of the garbage bin, if the segment features satisfy Eq. 12; otherwise, the segment is known as a non-vertical plane ($S_{bn,i}$).

$$S_{b,i} \rightarrow S_{bv,i} \, if \begin{cases} \angle n_{b,i} n_z \geq \alpha_{vo} \\ B.W_1/H_1 \leq S_{b,i}.W/L \leq B.W_2/H_2 \end{cases} \quad (4)$$

where α_{v0} = the maximum angle between vertical surfaces of the garbage bin and the oz axis.

Second, the non-vertical plane ($S_{bn,i}$) is considered as the ground plane $S_{bg,i}$ around the garbage bin (Eq. 13). This condition reflects the ground is located beneath a vertical plane.

$$S_{bn,i} \rightarrow S_{bg,i} \, if \begin{cases} \angle n_{bn,i} n_z \leq \alpha_{g,0} \\ p_{si}.z \leq p_{bv,i}.z_{min} + D.g_0 \end{cases} \quad (5)$$

where $p_{si}.z$ = z-coordinates of the points $p_{si} \in S_{bn,i}$
    $p_{bv,i}.z_{min}$ = the minimum z coordinate of $p_{bv,i} \in S_{bv,i}$

Third, as vertical planes of the garbage bin are above the ground plane, vertical planes ($S_{bv,i}$) are again filtered by examining the minimum distance from the points $p_{bv, i} \in S_{bv,i}$ to the ground plane $S_{bg, i}$ (Eq. 14). Notably, if the number of vertical planes ($S_{gv,i}$) is less than 2, the process is immediately terminated, and the sub-cell cluster R_i is discarded.

$$S_{bv,i} \rightarrow S_{bv,i} \, if \min\left(d(p_{bv,i}, S_g)\right) \leq D.g_o \quad (6)$$

Four, the vertical planes ($S_{bv,i}$) are vertical planes of the garbage bin if they connects together, which is determined by using connected surface component (CSC) analysis (Truong-Hong and Lindenbergh, 2022a). Two vertical planes ($S_{bv,i}$ and $S_{bv,j}$) are connected if Eq.s 15 and 16 are satisfied:

$$\angle n_{bv,i}, n_{bv,j} \geq \alpha_{s0} \quad (7)$$

$$\begin{cases} n_p \leq |p'_i| \, if \, d(p'_i, L_{ij}) \leq d_{buffer} \\ n_p \leq |p'_j| \, if \, d(p'_j, L_{ij}) \leq d_{buffer} \end{cases} \quad (8)$$
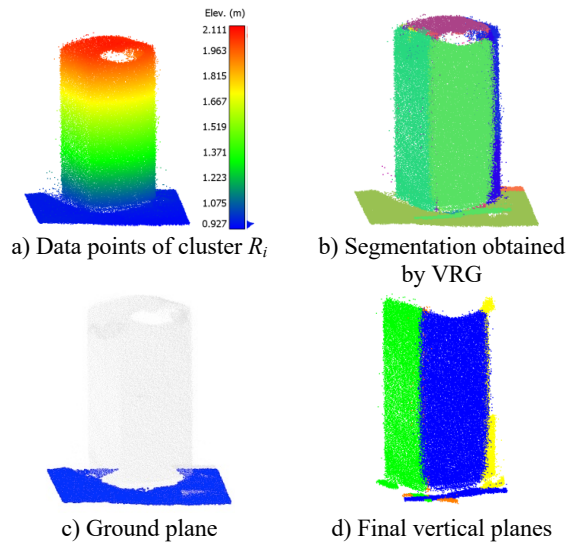
where $n_{bv,i}$ and $n_{bv,j}$ = normal vectors of $S_{bv,i}$ and $S_{bv,j}$
    α_{s0} = the minimum angle between two adjoined vertical planes of the public garbage bin
    L_{ij} = the intersection line between $S_{bv,i}$ and $S_{bv,j}$
    p'_i and p'_j = projected points of $p_{bv,i}$ and $p_{bv, j}$ onto $S_{bv,i}$ and $S_{bv,j}$, respectively.
    $d_{buffer} = 0.5B.W_{min}$ is a predefined threshold
    n_p = the minimum number of points
    $|\,\,|$ = the number of points

a) Data points of cluster R_i

b) Segmentation obtained by VRG

c) Ground plane

d) Final vertical planes

Figure 5. Extracting vertical planes of a bin

Subsequently, *Step 3.3* computes geometric characteristics of the garbage bin from its vertical surfaces, which consists of a primary dimensions (width – $B_i.W$, length – $B_i.L$, and height – $B_i.H$) and a secondary dimensions (area – $B_i.A = B_i.W \times B_i.L$, and an edge ratio – $B_i.R = B_i.W/B_i.L$). These features are computed from point clouds of cross-sections along the vertical direction, in which the number of sections and thickness of each section are empirically selected as $n_{sect} = 10$ and $t_{sect} = 0.02$ m. Finally, these features are

compared to ones derived from the design document to (1) identify if the candidate cluster is a real public garbage bin, and (2) then classify the Bin type.
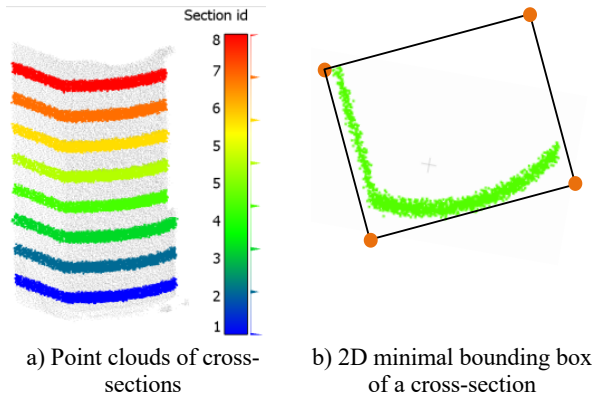

a) Point clouds of cross-sections   b) 2D minimal bounding box of a cross-section

Figure 6. Illustrate estimation of primary geometric dimensions of a candidate garbage bin

4. EXPERIMENTAL TEST, RESULTS AND DISCUSSIONS

To demonstrate the proposed method, MLS data of Rotterdam city, The Netherlands, were used. The data set was acquired for digitized urban streets of the Rotterdam city, from a MLS system consisting of 2 RIEGL VUX 1 laser scanners, and a Ladybug5 spherical image system of 30 MP. The RIEGL sensors can capture up to 1 million points per second with an accuracy of about 5mm. After processing data (e.g., data registration), a total of 166 tiles of LiDAR data was stored in LAZ format occupying 14.1 GB of storage. The data consists of a total of 2.84 billion points with x-, y-, and z-coordinates. Each tile covers an area of about 50m by 75m, while the number of points in a tile varies between 0.54 million and 66.6 million points (Figure 7). As the goal of the data acquisition was not meant for detecting public garbage bins, not all bins in the area are covered.
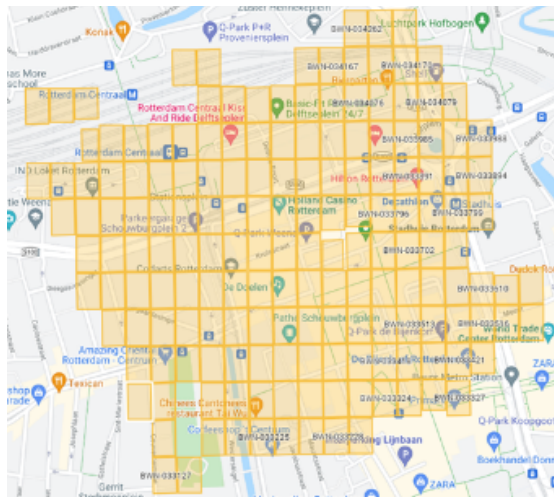

Figure 7. MLS data of the study area

Generally, MLS point clouds of a city are acquired in different trajectories, which require additional alignment in a common coordinate system. Although some alignment error is inevitable, there is considerable variation in this data set. For example, Figure 8 shows that the alignment errors of two tiles (two data files) are 4.4cm and 89 cm. This error can cause large deviations

of dimensions of recycle bins based on the point clouds compared to the design document. Therefore, lower and upper bounds of dimensions of the public garbage bin are empirically selected based on the design documents (Figure 1) with a tolerance of 25%.
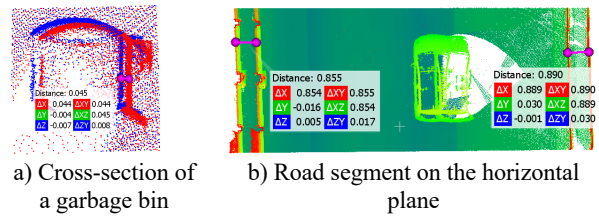

a) Cross-section of a garbage bin   b) Road segment on the horizontal plane

Figure 8. Data errors due to mis-alignment

As the proposed method combines spatial information from point clouds and contextual knowledge, input information consists of (1) x-, y- and z-coordinates of the point clouds, (2) lower and upper bounds of the dimensions of the garbage bins. Moreover, the set of input parameters used to process the point clouds can be divided into 3 main groups: (i) to extract candidate points of the public garbage bins (*Step 1 and 2),* (ii) to obtain final points of the surfaces of the garbage bins (*Step 3*), (iii) to check relative positions of surfaces of the garbage bins and the ground surface.

In this proposed method, each data tile is processed separately and in sequential order. Figure 9 illustrates the procedure of extraction of public garbage bins within the data tile. *Step 1 and 2* extract candidate points of the garbage bins from an entire data and then the final points of vertical surfaces of the garbage bin are obtained through *Step 3.*

Table 1. Input parameters used in the proposed method

Name	Notation	Value
(i) for extracting candidate points of public garbage bins		
Cell size	ce_0	1.0 m
Min. number of points of a cell	c_{min_ptc}	25 points
Sub-cell size	sce_0	0.1 m
Max. gap between two consecutive points in the vertical direction	$D.g_0$	0.1 m
(ii) for obtaining final points of surfaces of the garbage bins		
Voxel size	ve_0	0.15 m
Min. number of points of a voxel	v_{min_ptc}	5 points
Angle threshold	$v\alpha_0$	10^0
Distance threshold	vd_0	0.02 m
Residual threshold	$vres_0$	0.02 m
(iii) For checking relative positions of surfaces		
Max. angle of a ground surface	$\alpha_{g,0}$	10^0
Max. different height between adjoined sub-cells	ΔH_{sc}	0.3 m
The angle between vertical surfaces and the oz axis	α_{v0}	10^0
The minimum angle between two vertical planes	α_{s0}	45^0

An object-based strategy (Truong-Hong and Laefer, 2015) was employed to evaluate the quality of the public garbage bin extraction of the proposed method. An extracted garbage bin is considered as correct if its 2D footprint has more than 50% overlap to the ground truth. Moreover, the type of garbage bin is manually evaluated by comparing to the ground truth.

The study area has a total of 91 recycle bins including 44, 24, 18, 5 bins for Bin type 1, 2, 3 and 4, respectively, which was

manually extracted from the point cloud. The proposed method automatically processes MLS data points of 166 tiles to extract 92 garbage bins consisting of 47, 26, 14, and 5 for Bin type 1, 2, 3, and 4 (Figure 10). 10 of the extracted garbage bins were false extractions, while 7 garbage bins were classified into an incorrect type.
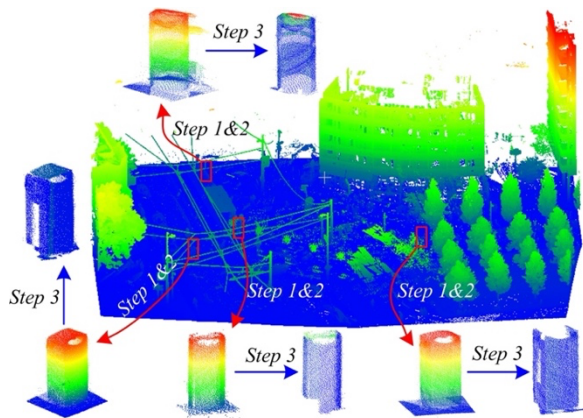

Figure 9. Recycle bin extraction from MLS data

Figure 10 shows the confusion matrix for extracting each type of public garbage bin. For the dominating Type 1 garbage bin, the proposed method detects bins with an accuracy of 0.872 and a F1-score of 0.932. however, the performance of detection is reduced for Type 2, for which the accuracy is 0.774. The main reason is that there is a high similarity between Type 1 and 2. Moreover, to consider overall detection, the proposed method extracts the public garbage bins with a detection rate of 89.1% (81 vs. 91).

Figure 10. Confusion matrix

Although a large data set was processed, the executing time for the entire data set was only about 163.6 minutes, in which *Step 2.1* and *Step 3.1* took respectively 90.2 minutes and 51.0 minutes. This running time is equivalent to 3.46 seconds per million points. Notably, the proposed method was implemented in Python and the experiment was processed on a Dell Precision

Workstation with the following main system configuration: Intel(R) Xeon(R) W-2123 CPU @ 3.6GHz with 32GB RAM.
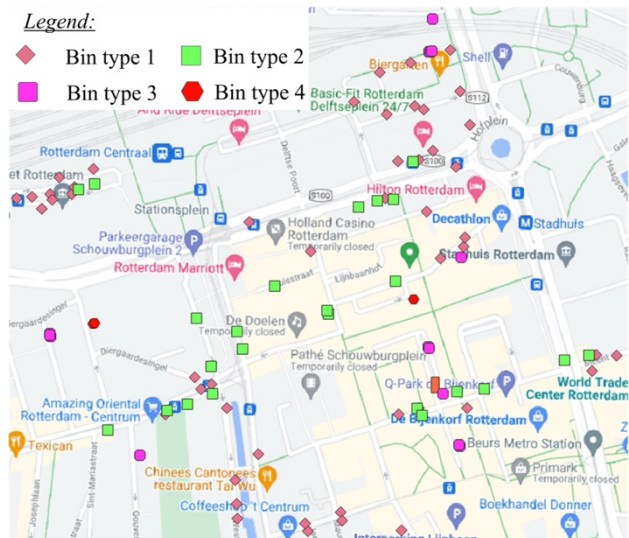

Figure 11. Positions of extracted public garbage bins overlaid on a Google map

Although the proposed method can extract garbage bins bin with an overall detection rate of 89.1%, results vary depending on the used input parameters. The size of sub-cell, and parameters for VRG (Table 2) have strong impact to results. The sub-cell size allows to separate vertical surfaces of the garbage bin from adjacent objects. For example, (Figure 12a), with a sub-cell size of 0.2m, the vertical surfaces of the garbage bin cannot be separated and the proposed method failed to recognize the garbage bin (Figure 12b). However, when a sub-cell size of 0.10m is used, the garbage bin is successfully detected (Figure 12c). The sub-cell size is selected mainly depending on the minimum distance between the recycle bin and adjacent objects, for example light poles, traffic barriers or bicycles.
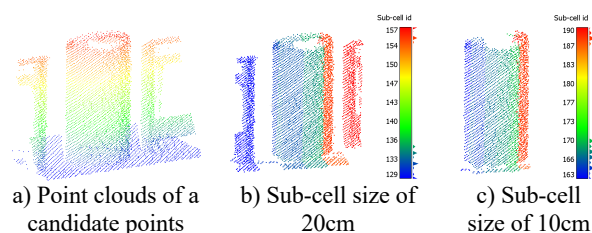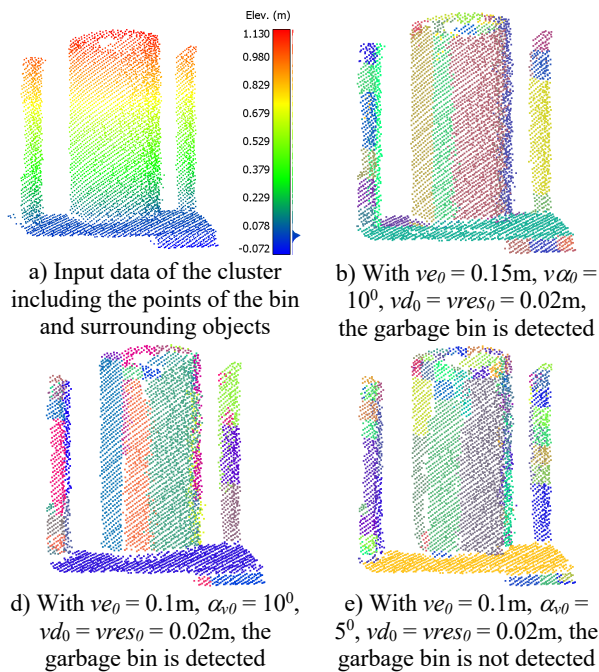

a) Point clouds of a candidate points b) Sub-cell size of 20cm c) Sub-cell size of 10cm

Figure 12. Impact of sub-cell size on extracted points of public garbage bins

Input parameters for VRG, including voxel size, and angle, distance and residual thresholds, also affect to quality of surface segmentation. Clearly, failure of extracting points of the garbage surfaces can lead to unsuccessful detection. The selecting voxel size mainly depends on the minimum size of the plane desired to extract, while the angle, distance and residual are strongly dominated by the data quality, e.g., noisy data or registration errors. For example, Figure 13 illustrates results of segmentation using VRG with various values of the voxel size, and angle, distance, and residual thresholds. With data quality of the dataset used in this study, the over-segmentation increased when the voxel size decreased from 0.15m (Figure 13b) to 0.1m (Figure 13c). Addition to decreasing the voxel size, the garbage bin is failed to detect when the angle threshold $v\alpha_0 = 5^0$ (Figure 13c).

a) Input data of the cluster including the points of the bin and surrounding objects

b) With $ve_0 = 0.15$m, $v\alpha_0 = 10^0$, $vd_0 = vres_0 = 0.02$m, the garbage bin is detected

d) With $ve_0 = 0.1$m, $\alpha_{v0} = 10^0$, $vd_0 = vres_0 = 0.02$m, the garbage bin is detected

e) With $ve_0 = 0.1$m, $\alpha_{v0} = 5^0$, $vd_0 = vres_0 = 0.02$m, the garbage bin is not detected

Figure 13. Impact of parameters for VRG on plane extraction to detect public garbage bins

5. CONCLUSIONS

To explore the ability to identify and assess relatively sparse urban objects from massive MLS data, this paper proposes a method to automatically extract points of urban recycle bins through three different filtering steps from cell to sub-cell to surface. The proposed method was tested on 2.84 MLS billion points, and extracted ~90 public garbage bins from an area of ~500.000 m^2 with an overall detection rate of 89.1%. The executing time for the entire dataset was about 163.6 minutes.

As MLS data acquisition was not designed to capture geometries of public garbage bins, data coverage and alignment errors strongly impact the resulting extraction and classification. Incomplete and/or sparse distribution of point clouds sometimes resulted in failures to detect surfaces of the garbage bins. The quality of point cloud alignment may lead to incorrect identification of the bins, as alignment issues may result in local deviations of design sizes.

REFERENCES

Bai, Q., Lindenbergh, R. C., Vijverberg, J. & Guelen, J. A. P. 2021. Road type classification of MLS point clouds using deep learning. *International Archives of the Photogrammetry, Remote Sensing and Spatial Information Sciences,* 43.

Edelsbrunner, H., Kirkpatrick, D. & Seidel, R. 1983. On the shape of a set of points in the plane. *IEEE Transactions on Information Theory,* 29**,** 551-559.

Guan, H., Yu, Y., Ji, Z., Li, J. & Zhang, Q. 2015. Deep learning-based tree classification using mobile LiDAR data. *Remote Sensing Letters,* 6**,** 864-873.

Laefer, D. F. & Truong-Hong, L. 2017. Toward automatic generation of 3D steel structures for building information modelling. *Automation in Construction,* 74**,** 66-77.

Liu, R., Wang, P., Yan, Z., Lu, X., Wang, M., Yu, J., Tian, M. & Ma, X. 2020. Hierarchical classification of pole-like objects in mobile laser scanning point clouds. *The Photogrammetric Record,* 35**,** 81-107.

Luo, H., Khoshelham, K., Chen, C. & He, H. 2021. Individual tree extraction from urban mobile laser scanning point clouds using deep pointwise direction embedding. *ISPRS Journal of Photogrammetry and Remote Sensing,* 175**,** 326-339.

Pu, S., Rutzinger, M., Vosselman, G. & Oude Elberink, S. 2011. Recognizing basic structures from mobile laser scanning data for road inventory studies. *ISPRS Journal of Photogrammetry and Remote Sensing,* 66**,** S28-S39.

Shi, Z., Kang, Z., Lin, Y., Liu, Y. & Chen, W. 2018. Automatic Recognition of Pole-Like Objects from Mobile Laser Scanning Point Clouds. *Remote Sensing,* 10.

Shirowzhan, S., Tan, W. & Sepasgozar, S. M. E. 2020. Digital Twin and CyberGIS for Improving Connectivity and Measuring the Impact of Infrastructure Construction Planning in Smart Cities. *ISPRS International Journal of Geo-Information,* 9.

Soilán, M., Riveiro, B., Martínez-Sánchez, J. & Arias, P. 2017. Segmentation and classification of road markings using MLS data. *ISPRS Journal of Photogrammetry and Remote Sensing,* 123**,** 94-103.

Tian, Y., Gelernter, J., Wang, X., Chen, W., Gao, J., Zhang, Y. & Li, X. 2018. Lane marking detection via deep convolutional neural network. *Neurocomputing,* 280**,** 46-55.

Truong-Hong, L. & Laefer, D. F. 2015. Quantitative evaluation strategies for urban 3D model generation from remote sensing data. *Computers & Graphics,* 49**,** 82-91.

Truong-Hong, L. & Lindenbergh, R. 2022a. Automatically extracting surfaces of reinforced concrete bridges from terrestrial laser scanning point clouds. *Automation in Construction,* 135**,** 104127.

Truong-Hong, L. & Lindenbergh, R. 2022b. Extracting structural components of concrete buildings from laser scanning point clouds from construction sites. *Advanced Engineering Informatics,* 51**,** 101490.

Wang, J., Lindenbergh, R. & Menenti, M. 2017. SigVox – A 3D feature matching algorithm for automatic street object recognition in mobile laser scanning point clouds. *ISPRS Journal of Photogrammetry and Remote Sensing,* 128**,** 111-129.

Wang, Z., Yang, L., Sheng, Y. & Shen, M. 2021. Pole-Like Objects Segmentation and Multiscale Classification-Based Fusion from Mobile Point Clouds in Road Scenes. *Remote Sensing,* 13.

Weinmann, M., Weinmann, M., Mallet, C. & Brédif, M. 2017. A Classification-Segmentation Framework for the Detection of Individual Trees in Dense MMS Point Cloud Data Acquired in Urban Areas. *Remote Sensing,* 9.

Wen, C., Sun, X., Li, J., Wang, C., Guo, Y. & Habib, A. 2019. A deep learning framework for road marking extraction, classification and completion from mobile laser scanning point

clouds. *ISPRS Journal of Photogrammetry and Remote Sensing,* 147**,** 178-192.

Yadav, M., Khan, P. & Singh, A. K. 2022. Identification of pole-like objects from mobile laser scanning data of urban roadway scene. *Remote Sensing Applications: Society and Environment,* 26**,** 100765.

Yadav, M., Singh, A. K. & Lohani, B. 2017. Extraction of road surface from mobile LiDAR data of complex road environment. *International Journal of Remote Sensing,* 38**,** 4655-4682.

Yang, M., Wan, Y., Liu, X., Xu, J., Wei, Z., Chen, M. & Sheng, P. 2018. Laser data based automatic recognition and maintenance of road markings from MLS system. *Optics & Laser Technology,* 107**,** 192-203.

Zai, D., Li, J., Guo, Y., Cheng, M., Lin, Y., Luo, H. & Wang, C. 2018. 3-D Road Boundary Extraction From Mobile Laser Scanning Data via Supervoxels and Graph Cuts. *IEEE Transactions on Intelligent Transportation Systems,* 19**,** 802-813.

Zhong, L., Cheng, L., Xu, H., Wu, Y., Chen, Y. & Li, M. 2017. Segmentation of Individual Trees From TLS and MLS Data. *IEEE Journal of Selected Topics in Applied Earth Observations and Remote Sensing,* 10**,** 774-787.

Zhou, M., Ma, L., Li, Y. & Li, J. Extraction of Building Windows from Mobile Laser Scanning Point Clouds. IGARSS 2018 - 2018 IEEE International Geoscience and Remote Sensing Symposium, 22-27 July 2018 2018. 4304-4307.